REPORT DOCUMENTATION PAGE

Form Approved
OMB NO. 0704-0188

1. AGENCY USE ONLY (Leave Blank)	2. REPORT DATE 12/12/2005	3. REPORT TYPE AND DATES COVERED Reprint

4. TITLE AND SUBTITLE
"Sound propagation through and scattering by internal gravity waves in a stably stratified atmosphere" Journal of the Acoustical Society of America, V. 118 (6) 3420-3429 (2005).

5. FUNDING NUMBERS
DAAD19-01-1-0640

6. AUTHOR(S)
V.E. Ostashev, I.P Chunchuzov, and D.K. Wilson

7. PERFORMING ORGANIZATION NAME(S) AND ADDRESS(ES)
Physics Department, New Mexico State University,
Box 30001, Dept. 3D, Las Cruces, NM 88003

8. PERFORMING ORGANIZATION REPORT NUMBER

9. SPONSORING / MONITORING AGENCY NAME(S) AND ADDRESS(ES)
U. S. Army Research Office
P.O. Box 12211
Research Triangle Park, NC 27709-2211

10. SPONSORING / MONITORING AGENCY REPORT NUMBER
42469.31-EV-H

11. SUPPLEMENTARY NOTES
The views, opinions and/or findings contained in this report are those of the author(s) and should not be construed as an official Department of the Army position, policy or decision, unless so designated by other documentation.

12 a. DISTRIBUTION / AVAILABILITY STATEMENT
Approved for public release; distribution unlimited.

12 b. DISTRIBUTION CODE

13. ABSTRACT (Maximum 200 words)
See the reprint attached.

14. SUBJECT TERMS

15. NUMBER OF PAGES
10

16. PRICE CODE

17. SECURITY CLASSIFICATION OR REPORT	18. SECURITY CLASSIFICATION ON THIS PAGE	19. SECURITY CLASSIFICATION OF ABSTRACT	20. LIMITATION OF ABSTRACT
UNCLASSIFIED	**UNCLASSIFIED**	**UNCLASSIFIED**	**UL**

Sound propagation through and scattering by internal gravity waves in a stably stratified atmosphere

Vladimir E. Ostashev
NOAA/Environmental Technology Laboratory, Boulder, Colorado 80305 and Department of Physics, New Mexico State University, Las Cruces, New Mexico 88003

Igor P. Chunchuzov
Obukhov Institute of Atmospheric Physics, Moscow, Russia

D. Keith Wilson
U.S. Army Engineer Research and Development Center, Hanover, New Hampshire 03755

(Received 8 March 2005; revised 28 September 2005; accepted 29 September 2005)

A stably stratified atmosphere supports propagation of internal gravity waves (IGW). These waves result in highly anisotropic fluctuations in temperature and wind velocity that are stretched in a horizontal direction. As a result, IGW can significantly affect propagation of sound waves in nighttime boundary layers and infrasound waves in the stratosphere. In this paper, a theory of sound propagation through, and scattering by, IGW is developed. First, 3D spectra of temperature and wind velocity fluctuations due to IGW, which were recently derived in the literature for the case of large wave numbers, are generalized to account for small wave numbers. The generalized 3D spectra are then used to calculate the sound scattering cross section in an atmosphere with IGW. The dependencies of the obtained scattering cross section on the sound frequency, scattering angle, and other parameters of the problem are qualitatively different from those for the case of sound scattering by isotropic turbulence with the von Kármán spectra of temperature and wind velocity fluctuations. Furthermore, the generalized 3D spectra are used to calculate the mean sound field and the transverse coherence function of a plane sound wave propagating through IGW. The results obtained also significantly differ from those for the case of sound propagation through isotropic turbulence. © *2005 Acoustical Society of America.* [DOI: 10.1121/1.2126938]

PACS number(s): 43.20.Fn, 43.28.Bj, 43.28.Lv [LCS] Pages: 3420–3429

I. INTRODUCTION

A stably stratified atmosphere often occurs in nighttime boundary layers (NBL) which extend from the ground to heights of about several hundred meters. Furthermore, the atmosphere is stably stratified in the stratosphere with the highest static stability in a range of heights from about 20 to 45 km.

A stably stratified atmosphere supports propagation of internal gravity waves (IGW). In NBL these waves can be trapped in a waveguide within a temperature inversion layer where the Brunt-Väisälä frequency is maximal. (The Brunt-Väisälä frequency is a characteristic frequency of IGW.[1]) The local maximum of this frequency near the stratopause (located about 45 km above the ground) can also be a barrier for IGW. In both cases, significant fluctuations in temperature T and wind velocity $\mathbf{v}$ are observed due to propagation of IGW.[1–4] These fluctuations are highly anisotropic and are stretched in a horizontal direction. The fluctuations can significantly affect sound propagation in NBL and infrasound propagation in the stratosphere. For example, facsimile records of sodars clearly show the presence of IGW in NBL (Refs. 1 and 2).

Despite the significance of sound propagation through, and scattering by, IGW, few theoretical studies of this phenomenon have been made. The reason for that is that such studies require combining results from two research topics: (1) 3D spectra of temperature and wind velocity fluctuations due to IGW in a stably stratified atmosphere; and (2) a general theory of sound propagation through, and scattering by, anisotropic turbulence with both temperature and wind velocity fluctuations. Significant progress in both research topics has been made only recently.

In the first of these research topics, 3D spectra of temperature and wind velocity fluctuations due to IGW were derived in Ref. 5 for the limiting case of large wave numbers (in comparison with the inverse outer scale of IGW). The spectra are very anisotropic: Their scale in a horizontal direction is much greater than that in a vertical direction. The 1D vertical spectra of temperature and wind velocity fluctuations obtained from these 3D spectra agree with those derived theoretically,[6,7] calculated numerically,[8,9] and measured in the stratosphere and troposphere, e.g., Refs. 3 and 10.

In the second research topic, a general theory of sound propagation through, and scattering by, anisotropic turbulence with temperature and wind velocity fluctuations has been developed in Refs. 11–14. Given the 3D spectra of T and $\mathbf{v}$ fluctuations, the theory provides formulas for calculations of the most widely used statistical moments of plane- and spherical sound waves: the sound scattering cross section, the variances and correlation functions of log-amplitude and phase fluctuations, the mean sound field, and the coherence function of the sound field.

The main goal of the present paper is to use the results obtained in these two research topics to develop a theory of sound propagation through, and scattering by, IGW. First, the 3D spectra of temperature and wind velocity fluctuations obtained in Ref. 5 for the case of large wave numbers are generalized to account for small wave numbers (of order of or smaller than the inverse outer scale of IGW). It is shown that the generalized 3D spectra have "realistic" 1D vertical spectra which, for large wave numbers, agree with those measured experimentally, and are bounded for small wave numbers.

Then, the generalized 3D spectra of temperature and wind velocity fluctuations are used to calculate the sound scattering cross section in the atmosphere with IGW. The obtained scattering cross section is compared with that due to sound scattering by isotropic turbulence with the von Kármán spectra of temperature and wind velocity fluctuations.

Furthermore, line-of-sight sound propagation through IGW with the 3D generalized spectra is studied. First, the extinction coefficient of the mean sound field is calculated. Then, the transverse coherence function of a plane sound wave is calculated and analyzed. The results obtained are also compared with those for the von Kármán spectra of temperature and wind velocity fluctuations.

The paper is organized as follows. In Sec. II, the spectra of temperature and wind velocity fluctuations due to IGW and von Kármán spectra of isotropic turbulence are considered. The sound scattering cross section in the atmosphere with IGW is calculated and analyzed in Sec. III. In Sec. IV, we consider line-of-sight sound propagation through IGW and calculate the mean sound field and the coherence function of a plane sound wave. The results obtained in the paper are summarized in Sec. V.

II. SPECTRA OF TEMPERATURE AND VELOCITY FLUCTUATIONS

A. 3D spectra for large wave numbers

At large wave numbers, the interaction between IGW modes is strongly nonlinear.[5–8] Such interaction transfers energy from random IGW sources to the modes with larger vertical and smaller horizontal scales than those in the source spectrum. This energy transfer is balanced by energy dissipation due to convective or shear instabilities at *very* large wave numbers.[15] As a result of the nonlinear interaction, 1D vertical spectra of temperature and horizontal wind velocity fluctuations have a universal form at large wave numbers that does not depend on the form of the spectrum for small wave numbers. These 1D vertical spectra have been studied extensively theoretically,[6,7] numerically,[8,9] and experimentally.[16–21]

However, when considering sound propagation through IGW, one needs to know 3D spectra of temperature and wind velocity fluctuations rather than 1D spectra. Using the mechanism of nonlinear interaction between IGW modes described above, the 3D spectra of temperature and horizontal wind velocity fluctuations were derived in Ref. 5. The 3D spectrum of temperature fluctuations is given by:

$$\Phi_T(\mathbf{K}) = \frac{AT_0^2N^4}{g^2|K_3|^5}\exp\left(-\frac{K_\perp^2}{4e_0K_3^2}\right), \tag{1}$$

where $\mathbf{K}=(K_1,K_2,K_3)$ is the turbulence wave vector, $K_\perp=\sqrt{K_1^2+K_2^2}$, N is the Brunt-Väisälä frequency, T_0 is the reference value of temperature, and g is the acceleration due to gravity. The components K_1, K_2, and K_3 of the turbulence wave vector are in the directions of the x-, y-, and z axes, with the z axis being vertical and the x- and y axes being in a horizontal plane. Furthermore, e_0 is a dimensionless parameter characterizing anisotropy of the spectrum. It is defined as a root-mean-square of the horizontal gradient of horizontal displacements due to IGW.[5,6] The value of e_0 depends on the degree of nonlinearity of IGW and can be in a wide range; however, e_0 is always much less than 1 (see the end of this section for more details). In Eq. (1), the numerical coefficient A is given by

$$A = \frac{\exp[-1/(32a_0)]}{2^{15}(2\pi)^{3/2}e_0a_0^{5/2}}. \tag{2}$$

Here, $a_0=M^2/8$, where M^2 is the mean-square vertical gradient of the vertical displacements due to IGW.[5] M characterizes the degree of nonlinearity of IGW and varies from 0 to about 0.5. (If $M>0.5$, IGW are unstable.) Therefore, in Eq. (2) the value of the parameter a_0 is in the range $0<a_0<0.03$.

Let $\Phi_{ij}(\mathbf{K})$ be the 3D spectral tensor of wind velocity fluctuations $\mathbf{v}=(v_1,v_2,v_3)=(v_x,v_y,v_z)$, where $i,j=1,2,3$. The theory developed in Ref. 5 results in isotropic velocity fluctuations in a horizontal plane so that $\Phi_{11}(\mathbf{K})=\Phi_{22}(\mathbf{K})$. Furthermore, $\Phi_{11}(\mathbf{K})$ has the same dependence on $\mathbf{K}$ as does the temperature spectrum

$$\Phi_{11}(\mathbf{K}) = \frac{AN^2}{2|K_3|^5}\exp\left(-\frac{K_\perp^2}{4e_0K_3^2}\right). \tag{3}$$

The vertical velocities due to IGW are significantly suppressed in comparison with the horizontal ones. Therefore, for the purpose of this paper, Φ_{i3} and Φ_{3i} can be ignored in comparison with Φ_{11}.

The 3D spectra of temperature and horizontal velocity fluctuations, Eqs. (1) and (3), were derived in Ref. 5 assuming that $K_3 \gg K_0$ and $K_3/K_0 \gg K_\perp/K_{0\perp}$. Here, K_0 and $K_{0\perp}$ are characteristic wave numbers of the spectra in vertical and horizontal directions, respectively, similar to the inverse outer scale of turbulence. Let $K_0=2\pi/L_0$, where L_0 is a characteristic spatial scale of the spectra. In NBL, $L_0\sim 300$ m, while in the stratosphere $L_0\sim 2-4$ km. $K_{0\perp}$ is much less than K_0 so that the ratio $\chi=K_0/K_{0\perp}$ is much greater than 1. Using the measurements of the vertical and horizontal velocities in NBL,[22] it can be shown that this ratio is in the range $3<\chi<10$. The range of values of χ in the stratosphere is not yet well known. Apparently, it can be as large as $\chi\sim 10$. This value of χ in the stratosphere will be assumed in numerical estimates below.

In Eqs. (1) and (3), the parameter e_0 is of the order of a_0/χ^2.[5] For the values of a_0 and χ given above, this parameter is in the range $0<e_0<3\cdot 10^{-3}$ in NBL, and in the range $0<e_0<3\cdot 10^{-4}$ in the stratosphere. Since $e_0 \ll 1$, the spectra

Φ_T and Φ_{11}, given by Eqs. (1) and (3), are very anisotropic: Their scale in a horizontal direction is much greater than that in the vertical direction.

Using the spectra Φ_T and Φ_{11}, given by Eqs. (1) and (3), the travel time fluctuations of sound propagation in NBL were calculated and compared with those measured experimentally.[23] The results obtained show good agreement between theoretical predictions and experimental data. This can be considered as an indirect experimental verification of the spectra (1) and (3). Note that direct measurements of the 3D spectra $\Phi_T(\mathbf{K})$ and $\Phi_{11}(\mathbf{K})$ are difficult to obtain; usually, 1D vertical spectra are measured experimentally by using different techniques, e.g., ground-based radars and lidars,[3,4,17] high-resolution radiosondes,[18,20] and measurements of stellar scintillations from space.[16] In the next section, starting from Eqs. (1) and (3), we derive 1D vertical spectra of temperature and wind velocity fluctuations, and discuss their agreement with experimental data and theoretical predictions.

B. 1D vertical spectra for large wave numbers

The 1D vertical spectrum $F_v(K_3)$ of temperature fluctuations is defined as

$$F_v(K_3) = \int_{-\infty}^{\infty} dK_1 \int_{-\infty}^{\infty} \Phi_T(K_1, K_2, K_3) dK_2. \tag{4}$$

Using this formula and Eq. (1) for Φ_T, the 1D vertical temperature spectrum can be calculated

$$F_v(K_3) = \frac{4\pi B e_0}{K_3^3}. \tag{5}$$

Here, $B = AT_0^2 N^4 / g^2$. Both the K_3^{-3} dependence and the coefficient $4\pi B e_0$ of the 1D vertical temperature spectrum, Eq. (5), agree with those measured experimentally in the stratosphere and troposphere.[3,4,16–19]

Using Eq. (3), it can be shown that the 1D vertical spectrum of v_x fluctuations is given by Eq. (5) if the constant B is replaced with $B' = AN^2/2$. It is shown in Refs. 5, 7, and 9 that the dependencies of this 1D vertical spectrum on K_3 and the coefficient $4\pi B' e_0$ are consistent with experimental data obtained in Refs. 10, 16, 20, and 21

The 1D vertical spectra of temperature and wind velocity fluctuations considered in this section also agree with those derived theoretically[6,21] and calculated numerically.[8,9]

C. Generalized 3D spectra

The spectrum Φ_T, given by Eq. (1), becomes unrealistic for small values of the vertical component of the turbulence wave vector, K_3. In this source region, Φ_T should be approximately constant. Therefore, it is worthwhile to generalize the spectrum (1) to account for small values of K_3.

In this paper, we propose the following generalization of the 3D temperature spectrum:

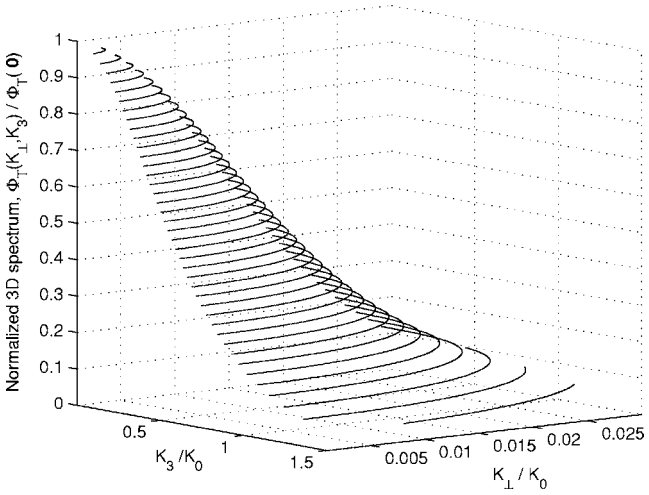

FIG. 1. The normalized generalized 3D spectrum of temperature fluctuations $\Phi_T(K_\perp, K_3)/\Phi_T(\mathbf{0})$. The anisotropy parameter is $e_0 = 10^{-4}$.

$$\Phi_T(\mathbf{K}) = \frac{AT_0^2 N^4}{g^2 (K_0^2 + K_3^2)^{5/2}} \exp\left(- \frac{K_\perp^2}{4 e_0 (K_0^2 + K_3^2)} \right). \tag{6}$$

If $K_3 \gg K_0$, the spectrum (6) coincides with that given by Eq. (1). If $K_3 \ll K_0$ and $K_\perp \ll 2\sqrt{e_0} K_0$, the spectrum (6) does not depend on $\mathbf{K}$ and is constant: $\Phi_T = AT_0^2 N^4 / (g^2 K_0^5)$. The suggested generalization of the spectrum (1) is similar to the generalization of the Kolmogorov spectrum when it is replaced by the von Kármán spectrum.[11,24] Note that the von Kármán spectra of temperature and wind velocity fluctuations have been widely used for studies of sound propagation through a turbulent atmosphere, e.g., see Refs. 11 and 25 and references therein.

The variance of temperature fluctuations is determined as

$$\sigma_T^2 = \int_{-\infty}^{\infty} dK_1 \int_{-\infty}^{\infty} dK_2 \int_{-\infty}^{\infty} \Phi_T(K_1, K_2, K_3) dK_3. \tag{7}$$

Substituting the value of Φ_T given by Eq. (6) into Eq. (7) and calculating the integrals, the constant A can be expressed in terms of σ_T^2

$$A = \frac{\sigma_T^2 g^2 K_0^2}{8\pi e_0 T_0^2 N^4}. \tag{8}$$

Using this value of A in Eq. (6), we obtain a desired form of the generalized 3D spectrum of temperature fluctuations

$$\Phi_T(\mathbf{K}) = \frac{K_0^2 \sigma_T^2}{8\pi e_0 (K_0^2 + K_3^2)^{5/2}} \exp\left(- \frac{K_\perp^2}{4 e_0 (K_0^2 + K_3^2)} \right). \tag{9}$$

Figure 1 shows $\Phi_T(K_\perp, K_3)$, given by this equation, normalized by $\Phi_T(\mathbf{0})$. In the figure, $e_0 = 10^{-4}$. It follows from Fig. 1 that $\Phi_T(K_\perp, K_3)$ reaches a maximum at $\mathbf{K} = 0$ and decreases along the $K_\perp$ axis (which corresponds to the horizontal components of the turbulence wave vector) much faster than along the K_3 axis (vertical components of the wave vector); i.e., the spectrum is highly anisotropic.

The proposed generalization of the 3D spectrum of horizontal velocity fluctuations, Eq. (3), is analogous to that of the 3D spectrum of temperature fluctuations

$$\Phi_{11}(\mathbf{K}) = \frac{AN^2}{2(K_0^2 + K_3^2)^{5/2}} \exp\left(- \frac{K_\perp^2}{4e_0(K_0^2 + K_3^2)} \right). \quad (10)$$

Thus, the generalized 3D spectra of temperature and wind velocity fluctuations, Eqs. (9) and (10), have the same dependence on $\mathbf{K}$ as do the corresponding spectra given by Eqs. (1) and (3).

The variance σ_v^2 of horizontal velocity fluctuations is given by a formula similar to Eq. (7): $\sigma_v^2 = \int \Phi_{11}(\mathbf{K}) d^3K$. Substituting Eq. (10) into this formula and calculating the integral over $\mathbf{K}$, we express the parameter A in terms of σ_v^2:

$$A = \frac{K_0^2 \sigma_v^2}{4\pi e_0 N^2}. \quad (11)$$

Using this value of A in Eq. (10), we obtain a desired form of the generalized 3D spectrum of horizontal velocity fluctuations

$$\Phi_{11}(\mathbf{K}) = \frac{K_0^2 \sigma_v^2}{8\pi e_0 (K_0^2 + K_3^2)^{5/2}} \exp\left(- \frac{K_\perp^2}{4e_0(K_0^2 + K_3^2)} \right). \quad (12)$$

Note that the variances of the temperature and horizontal velocity fluctuations in Eqs. (9) and (12) are related by a formula that can be obtained by eliminating the parameter A between Eqs. (8) and (11)

$$\sigma_v^2 = \frac{g^2}{2N^2} \frac{\sigma_T^2}{T_0^2}. \quad (13)$$

The generalized 3D spectra $\Phi_T(\mathbf{K})$ and $\Phi_{11}(\mathbf{K})$, given by Eqs. (9) and (12), will be used in Secs. III and IV for calculations of the statistical moments of a sound field propagating in an atmosphere with IGW.

D. Generalized 1D vertical spectra

In this section, we consider the generalized 1D temperature and horizontal velocity spectra. For the purpose of this section, it is more convenient to deal with Eqs. (6) and (10) for these spectra rather than with equivalent Eqs. (9) and (12).

Substituting Eq. (6) into Eq. (4) and calculating the integrals over K_1 and K_2, we obtain the generalized 1D vertical spectrum of temperature fluctuations

$$F_v(K_3) = \frac{4\pi B e_0}{(K_0^2 + K_3^2)^{3/2}}. \quad (14)$$

For $K_3 \gg K_0$, this spectrum coincides with that given by Eq. (5). Since the latter spectrum agrees with experimental data, so does the spectrum (14). For $K_3 \ll K_0$, the spectrum (14) is approximately constant. This is a more realistic behavior of the spectrum than an infinite increase of the spectrum (5) for small K_3.

It can be shown that the 1D vertical spectrum of horizontal velocity fluctuations is given by Eq. (14) if the constant B in this equation is replaced with the constant B'. This spectrum also agrees with experimental data for $K_3 \gg K_0$ and is approximately constant for $K_3 \ll K_0$.

E. von Kármán spectra of temperature and wind velocity fluctuations

The 3D von Kármán spectrum of isotropic temperature fluctuations is given by[11]

$$\Phi_T^{vK}(K) = \frac{2^{1/3}5}{3^{3/2}\Gamma^3(1/3)} \frac{K_T^{2/3} \sigma_{T,vK}^2}{(K_T^2 + K^2)^{11/6}}. \quad (15)$$

Here, K is the modulus of the turbulence wave number $\mathbf{K}$, Γ is the gamma function, $\sigma_{T,vK}^2$ is the variance of temperature fluctuations for the von Kármán spectrum, and K_T is a characteristic wave number inversely proportional to the outer scale of temperature fluctuations.

The 3D von Kármán spectral tensor of isotropic wind velocity fluctuations is given by[11]

$$\Phi_{ij}^{vK}(\mathbf{K}) = \frac{55}{2^{2/3}3^{5/2}\Gamma^3(1/3)} \left(\delta_{ij} - \frac{K_i K_j}{K^2} \right) \frac{K^2 K_v^{2/3} \sigma_{v,vK}^2}{(K_v^2 + K^2)^{17/6}}, \quad (16)$$

where δ_{ij} is the Kronecker symbol, $\sigma_{v,vK}^2$ is the variance of wind velocity fluctuations, and K_v is a characteristic wave number inversely proportional to the outer scale of velocity fluctuations.

Note that the von Kármán spectra $\Phi_T^{vK}(K)$ and $\Phi_{11}^{vK}(\mathbf{K})$ have different dependence on $\mathbf{K}$ even for $K \gg K_T$ and $K \gg K_v$, while the generalized 3D spectra given by Eqs. (9) and (12) have the same dependence.

III. SCATTERING OF SOUND BY IGW

The sound scattering cross section, σ, is an important statistical characteristic of a sound wave propagating in a medium with random inhomogeneities. In this section, we calculate σ for the case of sound scattering by IGW.

A. Sound scattering cross section

For anisotropic turbulence, the sound scattering cross section is given by[11]

$$\sigma = 2\pi k^4 \cos^2 \Theta \left[\frac{\Phi_T(\mathbf{q})}{4T_0^2} + \frac{n_{0,i} n_{0,j} \Phi_{ij}(\mathbf{q})}{c_0^2} \right]. \quad (17)$$

Here, k is the sound wave number, $\mathbf{q} = 2k(\mathbf{n}_0 - \mathbf{n})$ is the scattering vector, $\mathbf{n}_0 = (n_{0,1}, n_{0,2}, n_{0,3})$ is the unit vector in the direction of propagation of a sound wave incident on a scattering volume, $\mathbf{n}$ is the unit vector in the direction of propagation of a scattered wave, Θ is the scattering angle between the vectors $\mathbf{n}_0$ and $\mathbf{n}$, and summation is assumed over repeated subscripts.

In Eq. (17), it is worthwhile to express $\cos \Theta$ and $\mathbf{q}$ in terms of the spherical coordinates of the unit vectors $\mathbf{n}_0$ and $\mathbf{n}$. Without loss of generality, we assume that the vector $\mathbf{n}_0$ lies in the xz plane. Then, $\mathbf{n}_0 = (\sin \theta_0, 0, \cos \theta_0)$, where θ_0 is the angle between $\mathbf{n}_0$ and the vertical z axis; see Fig. 2. In the spherical coordinates, the unit vector $\mathbf{n}$ can be written as $\mathbf{n} = (\sin \theta \cos \phi, \sin \theta \sin \phi, \cos \theta)$. Here, θ is the angle between $\mathbf{n}$ and the vertical axis, and ϕ is the azimuthal angle between the projection of $\mathbf{n}$ on the horizontal plane and the x axis (Fig. 2).

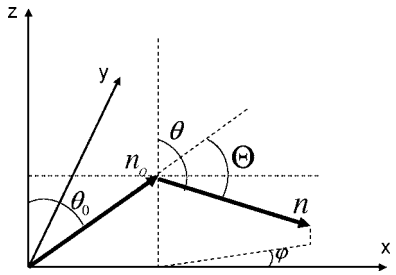

FIG. 2. The unit vectors $\mathbf{n}_0$ and $\mathbf{n}$ in the Cartesian coordinate system.

Using these representations of the unit vectors $\mathbf{n}_0$ and $\mathbf{n}$, the components of the scattering vector $\mathbf{q}=(q_1,q_2,q_3)$ can be expressed in terms of the spherical coordinates of $\mathbf{n}_0$ and $\mathbf{n}$

$$q_1 = 2k(\sin\theta_0 - \sin\theta\cos\phi), \quad q_2 = -2k\sin\theta\sin\phi,$$

$$q_3 = 2k(\cos\theta_0 - \cos\theta). \tag{18}$$

Furthermore, $\cos\Theta=\mathbf{n}_0\cdot\mathbf{n}$ can be written as

$$\cos\Theta = \sin\theta_0\sin\theta\cos\phi + \cos\theta_0\cos\theta. \tag{19}$$

Since $n_{0,2}=0$ in Eq. (17), the terms proportional to Φ_{i2} and Φ_{2j} do not contribute to σ. Furthermore, the terms proportional to Φ_{i3} and Φ_{3j} are much less than the term proportional to Φ_{11} if the angle θ_0 is not too small. If $\theta_0=0$, the terms proportional to Φ_{i3} and Φ_{3j} are small in comparison with the term proportional to Φ_T for most "reasonable" values of N.

Thus, in Eq. (17), the sum $n_{0,i}n_{0,j}\Phi_{ij}$ can be approximated as $\sin^2\theta_0\Phi_{11}$. Furthermore, in this equation, we replace Φ_T and Φ_{11} by their values given by Eqs. (9) and (12), respectively. Finally, using Eq. (18), we obtain a desired formula for the scattering cross section due to sound scattering by IGW

$$\sigma = \frac{K_0^2\cos^2\Theta\exp\left\{-\dfrac{\sin^2\theta_0+\sin^2\theta-2\sin\theta_0\sin\theta\cos\phi}{4e_0[K_0^2/(4k^2)+(\cos\theta_0-\cos\theta)^2]}\right\}}{2^9 e_0 k[K_0^2/(4k^2)+(\cos\theta_0-\cos\theta)^2]^{5/2}} \times\left[\frac{\sigma_T^2}{T_0^2}+4\sin^2\theta_0\frac{\sigma_v^2}{c_0^2}\right]. \tag{20}$$

It is worthwhile to compare the obtained value of σ with that for the case of sound scattering by isotropic temperature and wind velocity fluctuations with the von Kármán spectra. The latter scattering cross section was calculated in Ref. 26

$$\sigma_{vK} = \frac{b_1 k^{1/3}K_T^{2/3}\cos^2\Theta}{[K_T^2/(4k^2)+\sin^2(\Theta/2)]^{11/6}} \times\left[\frac{\sigma_{T,vK}^2}{T_0^2}+\frac{11\sin^2\Theta}{6[K_T^2/(4k^2)+\sin^2(\Theta/2)]}\frac{\sigma_{v,vK}^2}{c_0^2}\right]. \tag{21}$$

Hereinafter, for simplicity, $K_T=K_v$. Furthermore, in Eq. (21) and for some equations below, involved numerical coefficients are denoted by b with subscripts; in Eq. (21) $b_1=5\pi/(2^{13/3}3^{3/2}\Gamma^3(1/3))=0.0078$.

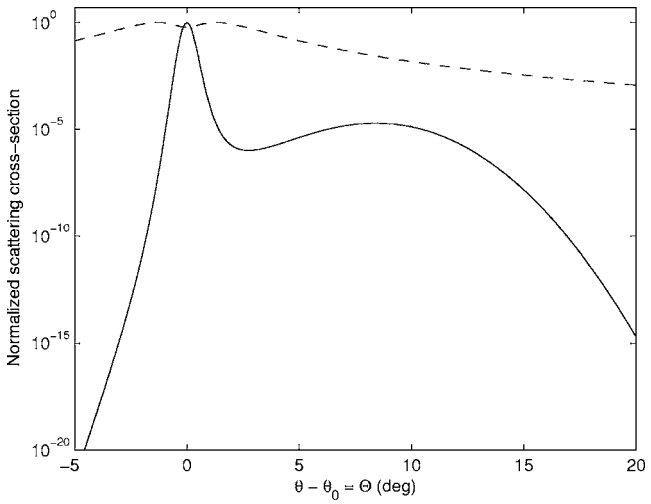

FIG. 3. The normalized scattering cross section versus the difference $\theta-\theta_0=\Theta$. For this plot, the sound frequency $f=3$ Hz, the anisotropy parameter $e_0=10^{-4}$, the angle $\theta_0=85°$, and the scale $L_0=3$ km. The solid and dashed lines correspond to σ and σ_{vK}, respectively, normalized by their maximum values.

B. Analysis

Let us compare the sound scattering cross sections σ and σ_{vK} given by Eqs. (20) and (21), respectively. In atmospheric acoustics, the terms $K_0^2/(4k^2)$ and $K_T^2/(4k^2)$ appearing in these equations are both small and can be neglected for most geometries of scattering.

There are several differences between σ and σ_{vK}. First, σ_{vK} depends only on the scattering angle Θ between the unit vectors $\mathbf{n}_0$ and $\mathbf{n}$, as must be the case for scattering by isotropic turbulence, while σ depends not only on Θ but also on the orientation of these unit vectors. Second, σ and σ_{vK} have different dependencies on the frequency $f=kc_0/(2\pi)$ of a sound wave: If $K_0^2/(4k^2)$ and $K_T^2/(4k^2)$ can be neglected in Eqs. (20) and (21), $\sigma\sim 1/f$ while $\sigma_{vK}\sim f^{1/3}$. Third, in Eqs. (20) and (21) the factors in front of the terms σ_v^2/c_0^2 and $\sigma_{v,vK}^2/c_0^2$ are different. Therefore, relative contributions to σ and σ_{vK} due to sound scattering by temperature and velocity fluctuations are different.

Finally, let us compare the dependence of the sound scattering cross sections σ and σ_{vK} on the scattering angle Θ. In Fig. 3, the solid curve corresponds to the dependence of σ, normalized by its maximum value, on the difference $\theta-\theta_0$. When plotting this curve, it was assumed that $\sigma_T^2/T_0^2=\sigma_v^2/c_0^2$, $e_0=10^{-4}$, $\theta_0=85°$, $f=3$ Hz, and $L_0=3$ km. (The numerical value of L_0 corresponds to IGW in the stratosphere; see Sec. II A.) Furthermore, it was assumed that the azimuthal angle $\phi=0$. In this case, both $\mathbf{n}_0$ and $\mathbf{n}$ lie in the xz plane (see Fig. 2) so that the difference $\theta-\theta_0$ is equal to the scattering angle Θ. The dashed curve in Fig. 3 corresponds to the dependence of σ_{vK}, also normalized by its maximum value, on the scattering angle Θ. When plotting the dashed curve, we assumed that $\sigma_{T,vK}^2/T_0^2=\sigma_{v,vK}^2/c_0^2$, $K_T=K_0$, and, as for the solid curve, $f=3$ Hz.

Figure 3 shows two maxima in the dependence of σ on $\theta-\theta_0=\Theta$. The first maximum occurs at $\theta=\theta_0$ (i.e., at $\Theta=0$) and corresponds to forward scattering of a sound wave. The appearance of this maximum is well known in theories of

sound scattering by isotropic turbulence: σ_{vK} reaches its maximum values for predominantly forward scattering. (In Fig. 3, a small dip in the dashed curve at $\Theta=0$ is due to the fact that sound scattering by isotropic velocity fluctuations is zero at $\Theta=0$; this dip would disappear for the case of sound scattering by only temperature fluctuations.) The second, much broader maximum in the dependence of σ on Θ occurs at $\Theta=\pi-2\theta_0=10°$. This maximum occurs in the direction of specular reflection of the incident wave from a horizontal plane. The appearance of this maximum is due to the fact that random inhomogeneities in temperature and wind velocity are highly stretched in horizontal planes, effectively producing a random layered medium. A plane wave incident on such a random layered medium is transmitted through, and reflected from, the medium. The transmitted and reflected waves correspond to two maxima in the solid curve in Fig. 3. Note that the dashed curve in this figure does not have a maximum at $\Theta=10°$.

The second maximum in the solid curve in Fig. 3 can explain an interesting phenomenon in infrasound propagation occurring at heights of about 35–45 km. The infrasound waves are often partially "reflected" from these heights even though the effective sound speed in the stratosphere is less than that near the ground, which prevents such reflection in geometrical acoustics.[27] The second maximum in the dependence of σ on Θ occurs at $\theta=105°$, i.e., when the scattered wave propagates back to the ground. Therefore, Fig. 3 shows that a significant portion of infrasound energy can be scattered back to the ground from the stratosphere.

C. Backscattering

An important particular case of sound scattering in the atmosphere is backscattering, which occurs for $\Theta=180°$. The backscattering cross section $\sigma(\Theta=180°)$ can be measured by monostatic sodars.[28,29]

For the case of backscattering, Eq. (20) can be simplified by taking into account that $\mathbf{n}=-\mathbf{n}_0$, $\theta=\pi-\theta_0$, and $\phi=\pi$. As a result, we obtain the following formula for the backscattering cross section due to sound scattering by IGW:

$$\sigma(180°)=\frac{K_0^2\exp\left\{-\dfrac{\sin^2\theta_0}{4e_0[K_0^2/(16k^2)+\cos^2\theta_0]}\right\}}{2^{14}e_0k[K_0^2/(16k^2)+\cos^2\theta_0]^{5/2}}\times\left[\frac{\sigma_T^2}{T_0^2}+4\sin^2\theta_0\frac{\sigma_v^2}{c_0^2}\right]. \tag{22}$$

For the von Kármán spectra of temperature and velocity fluctuations, the backscattering cross section is given by

$$\sigma_{vK}(180°)=\frac{b_1k^{1/3}K_T^{2/3}}{[1+K_T^2/(4k^2)]^{11/6}}\frac{\sigma_{T,vK}^2}{T_0^2}. \tag{23}$$

It follows from Eqs. (22) and (23) that velocity fluctuations can contribute to $\sigma(180°)$; however, they do not contribute to $\sigma_{vK}(180°)$. Furthermore, $\sigma(180°)$ significantly depends on θ_0 while $\sigma_{vK}(180°)$ does not.

Figure 4 shows the dependence of $\sigma(180°)$ (normalized by its value at $\theta_0=0$) on the angle θ_0 for different values of e_0: 3×10^{-4}—dash-dotted line; 10^{-3}—dashed line; and 3×10^{-3}—solid line. When plotting Fig. 4, it was assumed that $f=3$ kHz and $L_0=300$ m. (The numerical value of L_0 corresponds to IGW in NBL, see Sec. II A.) It follows from Fig. 4 that the backscattering cross section decreases rapidly with the increase of the angle θ_0. One would expect such dependence of $\sigma(180°)$ on θ_0 for a layered random medium.

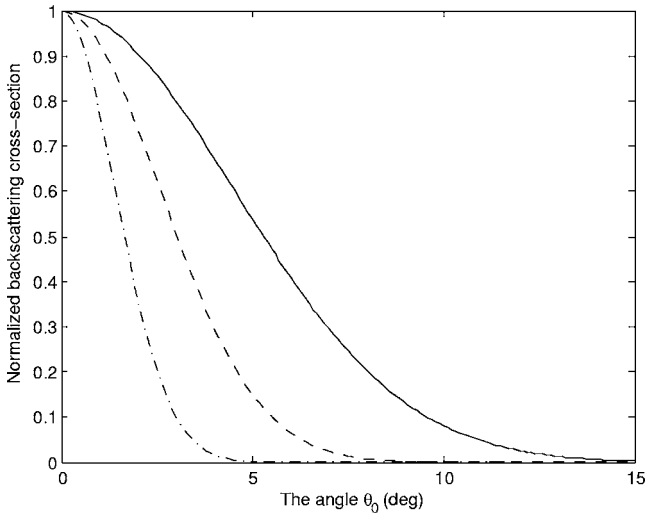

FIG. 4. The normalized backscattering cross section versus the angle θ_0. Dash-dotted line corresponds to $e_0=3\times10^{-4}$, dashed line to $e_0=10^{-3}$, and solid line to $e_0=3\times10^{-3}$. For this figure, the sound frequency $f=3$ kHz and the scale $L_0=300$ m.

IV. LINE-OF-SIGHT SOUND PROPAGATION THROUGH IGW

In this section, we will consider line-of-sight sound propagation in an atmosphere with temperature and wind velocity fluctuations induced by IGW. We will assume that a sound wave propagates nearly horizontally in the direction of the x axis. This is a reasonable assumption for many problems of atmospheric acoustics, e.g., for near-ground sound propagation.

A. Effective 3D spectrum

A theory of line-of-sight sound propagation through anisotropic, inhomogeneous turbulence with temperature and wind velocity fluctuations has been recently developed in Refs. 12–14. Using the Markov approximation and the Rytov or parabolic equation method, formulas for the variances and correlation functions of log-amplitude and phase fluctuations, the mean field, and the coherence function of plane and spherical sound waves were derived. These statistical moments of a sound field were expressed in terms of the effective 3D spectral density of random inhomogeneities[11–14]

$$\Phi_{\text{eff}}(\mathbf{K})=\frac{\Phi_T(\mathbf{K})}{T_0^2}+\frac{4\Phi_{11}(\mathbf{K})}{c_0^2}. \tag{24}$$

Using Eqs. (9) and (12), the effective 3D spectral density can be calculated for the case of sound propagation through IGW

$$\Phi_{\text{eff}}(\mathbf{K}) = \frac{K_0^2 \exp\left[-\dfrac{K_\perp^2}{4e_0(K_0^2+K_3^2)}\right]}{8\pi e_0 (K_0^2+K_3^2)^{5/2}} \left[\frac{\sigma_T^2}{T_0^2} + 4\frac{\sigma_v^2}{c_0^2}\right]. \quad (25)$$

Using this formula for $\Phi_{\text{eff}}(\mathbf{K})$ and equations obtained in Refs. 12–14, the above-mentioned statistical moments of plane- and spherical sound waves propagating through IGW can be readily calculated. In this section, we will calculate and analyze the mean sound field and the coherence function of a plane sound wave.

B. Mean sound field

The mean field $\langle p \rangle$ of a sound wave propagating in a random medium attenuates exponentially[11]

$$\langle p(\mathbf{R}) \rangle = p_0(\mathbf{R}) e^{-\gamma x}. \quad (26)$$

Here, $\mathbf{R}=(x,y,z)$, p_0 is the sound field in the absence of random inhomogeneities, x in the exponent indicates the distance of sound propagation in a turbulent atmosphere, and γ is the extinction coefficient given by[14]

$$\gamma = \frac{\pi k^2}{4} \int_{-\infty}^{\infty} dK_2 \int_{-\infty}^{\infty} \Phi_{\text{eff}}(0,K_2,K_3) dK_3. \quad (27)$$

The extinction coefficient γ is an important statistical characteristic of a field propagating in a random medium. It indicates the rate at which the coherent part of the field is transformed into the incoherent one.

Substituting the value of Φ_{eff} from Eq. (25) into Eq. (27), and calculating the integrals over K_2 and K_3, we obtain the following formula for the extinction coefficient of the mean sound field propagating through IGW:

$$\gamma = \frac{b_2 k^2}{\sqrt{e_0} K_0} \left[\frac{\sigma_T^2}{T_0^2} + 4\frac{\sigma_v^2}{c_0^2}\right], \quad (28)$$

where $b_2 = \pi^{3/2}/32 \cong 0.174$.

Let us compare Eq. (28) with the extinction coefficient γ_{vK} of the mean sound field propagating in a turbulent atmosphere with the von Kármán spectra of temperature and velocity fluctuations, which can be obtained with the use of Eqs. (7.110) and (7.111) from Ref. 11

$$\gamma_{vK} = \frac{b_3 k^2}{K_T} \left[\frac{\sigma_{T,vK}^2}{T_0^2} + 4\frac{\sigma_{v,vK}^2}{c_0^2}\right]. \quad (29)$$

Here, $b_3 = \pi^2/(2^{2/3}\sqrt{3}\Gamma^3(1/3)) \cong 0.187$. It follows from Eqs. (28) and (29) that the dependencies of γ and γ_{vK} on the parameters of the problem are similar with one exception: The denominator in Eq. (28) contains a small factor $\sqrt{e_0}$.

The inverse of the extinction coefficient, γ^{-1}, is equal to the distance x of sound propagation in a random medium at which the mean sound field has decayed by a factor $1/e$. It follows from Eq. (28) that $\gamma^{-1} = \sqrt{e_0} c_0^2/(2\pi b_2 f^2 M)$, where $M = L_0(\sigma_T^2/T_0^2 + 4\sigma_v^2/c_0^2)$ is the outer scale-variance product. The values of γ^{-1} versus f and M are depicted in Fig. 5(a). Similarly, it can be shown from Eq. (29) that $\gamma_{vK}^{-1} = c_0^2/(2\pi b_3 f^2 M_{vK})$, where $M_{vK} = L_T(\sigma_{T,vK}^2/T_0^2 + 4\sigma_{v,vK}^2/c_0^2)$ is the outer scale-variance product for the von Kármán spectra. Here, $L_T = 2\pi/K_T$. Figure 5(b) shows γ_{vK}^{-1} as a function of f and M_{vK}. Figures 5(a) and 5(b) give us typical values of γ^{-1} and γ_{vK}^{-1} in the atmosphere. It also follows from these figures that $\gamma^{-1} \ll \gamma_{vK}^{-1}$ provided that $M = M_{vK}$.

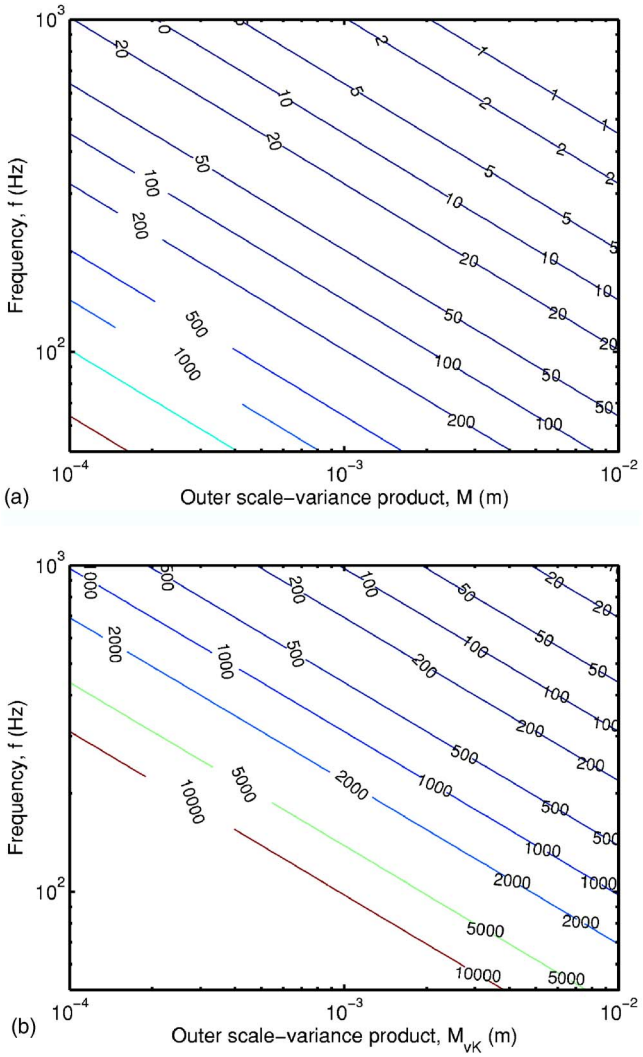

FIG. 5. (Color online) (a) The inverse of the extinction coefficient, γ^{-1}, for IGW as a function of the frequency f and the outer scale-variance product $M = L_0(\sigma_T^2/T_0^2 + 4\sigma_v^2/c_0^2)$. The values of γ^{-1} are in meters. For this plot, $e_0 = 4 \times 10^{-4}$. (b) The inverse of the extinction coefficient, γ_{vK}^{-1}, for the von Kármán spectra as a function of the frequency f and the outer scale-variance product $M_{vK} = L_T(\sigma_{T,vK}^2/T_0^2 + 4\sigma_{v,vK}^2/c_0^2)$. The values of γ_{vK}^{-1} are in meters.

C. Coherence function of a plane sound wave

Let the two points of observation (x, y_1+y, z_1+z) and (x, y_1, z_1) be located in a plane perpendicular to the x axis. Here, y and z are the distances between these two points along the y- and z axes. The transverse coherence function of a sound field p is determined by

$$\Gamma(x;y,z) = \langle p(x, y_1+y, z_1+z) p^*(x, y_1, z_1) \rangle. \quad (30)$$

For the considered case of plane-wave propagation, the transverse coherence function does not depend on the coordinates y_1 and z_1; e.g., see Ref. 30.

In Ref. 14, the following formula for Γ was derived:

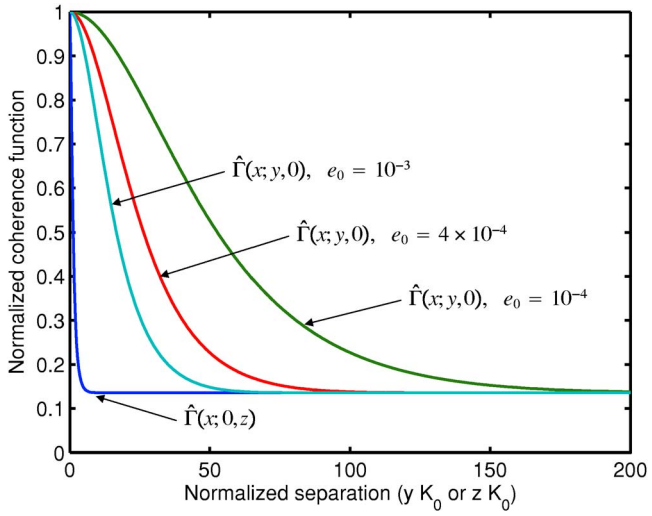

FIG. 6. (Color online) The normalized coherence function $\hat{\Gamma}(x;y,z)$ of a plane sound wave propagating through IGW. The curves show this function for $x=\gamma^{-1}$ and for either a vertical separation ($y=0$) or a horizontal separation ($z=0$) between two points of observation. The abscissa is yK_0 for horizontal separations or zK_0 for vertical separations. Three curves are shown for horizontal separations, which correspond to $e_0=10^{-4}$, $e_0=4\times10^{-4}$, and $e_0=10^{-3}$.

$$\Gamma(x;y,z)=|A_0^2|\exp\left\{-\frac{\pi k^2 x}{2}\int_{-\infty}^{\infty}dK_2 \times\int_{-\infty}^{\infty}[1-e^{i(yK_2+zK_3)}]\Phi_{\text{eff}}(0,K_2,K_3)\right\}dK_3. \tag{31}$$

Here, A_0 is the amplitude of the plane sound wave at $x=0$. After substituting the expression for Φ_{eff} given by Eq. (25) into Eq. (31), some algebra yields a formula for the coherence function of a plane sound wave propagating through IGW

$$\Gamma(x;y,z)=|A_0^2|\exp[-x\gamma F(y,z)]. \tag{32}$$

Here, the function F characterizes the dependence of the coherence function on y and z

$$F(y,z)=\frac{4}{\pi}\int_{-\infty}^{\infty}\frac{1-\exp[izK_0\xi-e_0y^2K_0^2(1+\xi^2)]}{(1+\xi^2)^2}d\xi. \tag{33}$$

Figure 6 shows the normalized coherence function of a plane sound wave $\hat{\Gamma}(x;y,z)=\Gamma(x;y,z)/|A_0^2|$ calculated with the use of Eqs. (32) and (33). The calculations were made for $x\gamma=1$ and three values of e_0. Results for both vertical ($y=0$) and horizontal ($z=0$) separations between two points of observation are shown. The coherence is observed to decay much more rapidly with increasing vertical separation than with increasing horizontal separation. This trend is enhanced for smaller values of e_0.

It is also worthwhile to consider two limiting cases when analytical formulas for $\Gamma(x;y,z)$ can be obtained. In the first limiting case, the values of y and z are relatively large

$$zK_0\gg1,\quad e_0y^2K_0^2\gg1. \tag{34}$$

It can be shown that, in this case, $F\approx2$, so that

$$\Gamma(x;y,z)=|A_0^2|\exp(-2x\gamma). \tag{35}$$

This formula represents the correct asymptotic behavior of the coherence function for relatively large distances between the observation points. Indeed, in this case $p(x,y_1+y,z_1+z)$ and $p^*(x,y_1,z_1)$ do not correlate, so that Eq. (30) takes the form: $\Gamma(x;y,z)=\langle p(x,y_1+y,z_1+z)\rangle\langle p^*(x,y_1,z_1)\rangle$. Replacing $\langle p\rangle$ and $\langle p^*\rangle$ in this formula with their values given by Eq. (26) results in Eq. (35). Note that, for $x\gamma=1$, it follows from Eq. (35) that $\Gamma(x;y,z)/|A_0^2|=1/e^2$. This result is in agreement with Fig. 6, where all four curves reach their asymptote $1/e^2$ for large values of y or z.

Let $\Gamma_{vK}(x;r)$ be the coherence function of a plane sound wave for the case of the von Kármán spectra of temperature and velocity fluctuations, where $r=\sqrt{y^2+z^2}$. The value of $\Gamma_{vK}(x;r)$ is given by Eq. (7.112) from Ref. 11. It can be shown that, if $rK_T\gg1$ [which is similar to inequalities Eq. (34)], Γ_{vK} is given by Eq. (35) if γ is replaced with γ_{vK}.

Let us now consider the other limiting case of $\Gamma(x;y,z)$ when the values of y and z are relatively small

$$zK_0\ll1,\quad e_0y^2K_0^2\ll1. \tag{36}$$

It can be shown that, in this case, $F\approx4e_0y^2K_0^2+z^2K_0^2$. Substituting this value of F into Eq. (32), we obtain

$$\Gamma(x;y,z)=|A_0^2|\exp[-x\gamma(4e_0y^2K_0^2+z^2K_0^2)]. \tag{37}$$

If $rK_T\ll1$ [which is similar to Eq. (36)], $\Gamma_{vK}(x;r)$ can also be simplified

$$\Gamma_{vK}(x;r)=|A_0^2|\exp(-b_4\eta x\gamma_{vK}K_T^{5/3}r^{5/3}). \tag{38}$$

Here, $b_4=3^{3/2}\Gamma^3(1/3)/(2^{1/3}5\Gamma(2/3)\pi)\cong3.73$, and the numerical coefficient η is given by

$$\eta=\frac{\sigma_{T,vK}^2/T_0^2+(22/3)\sigma_{v,vK}^2/c_0^2}{\sigma_{T,vK}^2/T_0^2+4\sigma_{v,vK}^2/c_0^2}. \tag{39}$$

This coefficient depends on the values of the variances of the temperature and velocity fluctuations for the von Kármán spectra, $\sigma_{T,vK}^2$ and $\sigma_{v,vK}^2$, and varies in the range $1\leqslant\eta\leqslant11/6$.

The most noticeable difference between the coherence functions given by Eqs. (37) and (38) is that $\Gamma(x;y,z)$ is a highly anisotropic function of the coordinates y and z, while $\Gamma_{vK}(x;r=\sqrt{y^2+z^2})$ is an isotropic function of these coordinates. Furthermore, in Eq. (37) y and z are both squared, while in Eq. (38) they have a different power.

D. Coherence radius

The coherence radius is an important characteristic of the coherence function. It indicates the distance between the two points of observation at which the coherence function decreases by a factor of e^{-1}.

Let us consider the limiting case of relatively small values of y and z when Eq. (36) holds and when the coherence radius can be determined analytically. In this case, the coherence radius y_c along the y axis can be determined by setting $z=0$ and equating the exponential term in Eq. (37) to e^{-1}

$$y_c = \frac{1}{2K_0\sqrt{e_0\gamma x}}. \tag{40}$$

Similarly, setting $y=0$, we obtain the coherence radius z_c along the z axis

$$z_c = \frac{1}{K_0\sqrt{\gamma x}}. \tag{41}$$

Comparing Eqs. (40) and (41) reveals that the coherence radius along the y axis is much greater than that along the z axis: $y_c = z_c/(2\sqrt{e_0})$. Since y and z must satisfy Eq. (36), the coherence radii y_c and z_c exist if $\gamma x > 1$.

Using the formula Eq. (38) for $\Gamma_{vK}(x;r)$, it can be shown that, for $rK_T \ll 1$, the coherence radii $y_{c,vK}$ and $z_{c,vK}$ for the von Kármán spectra of temperature and wind velocity fluctuations are given by

$$y_{c,vK} = z_{c,vK} = \frac{1}{K_T(b_4\eta x\gamma_{vK})^{3/5}}. \tag{42}$$

Comparing Eqs. (40)–(42) reveals that, for the case of sound propagation through IGW, the coherence radii have a different power dependence on the propagation distance and extinction coefficient than those for the case of the von Kármán spectra of temperature and velocity fluctuations.

V. CONCLUSIONS

In this paper, we have developed a theory of sound propagation through, and scattering by, IGW in a stably stratified atmosphere.

First, the 3D spectra of temperature and horizontal wind velocity fluctuations due to IGW recently developed in Ref. 5 for the case of large wave numbers were generalized to account for small wave numbers. The variances of temperature and wind velocity fluctuations of the generalized 3D spectra were calculated.

Then, the generalized 3D spectra of temperature and wind velocity fluctuations were used to study sound scattering by IGW. A formula for the sound scattering cross section σ was derived. It was shown that σ has different dependencies on the sound frequency, scattering angle, and other parameters of the problem than does the scattering cross section due to sound scattering by temperature and wind velocity fluctuations with the von Kármán spectra. Furthermore, the scattering cross section σ has two maxima as a function of the scattering angle. The first maximum occurs in the direction of propagation of a sound wave incident on the scattering volume. The second maximum appears in the direction at which the incident sound wave would be specularly reflected from a horizontal plane. This second maximum is due to the fact that temperature and wind velocity fluctuations induced by IGW are highly stretched in a horizontal direction. The second maximum can explain the interesting phenomenon of a partial infrasound "reflection" from the stratosphere which is observed experimentally.

The generalized 3D spectra of temperature and wind velocity fluctuations were also used to study line-of-sight sound propagation through an atmosphere with IGW. The extinction coefficient γ of the mean sound field was calculated and compared with that for the case of sound propagation through isotropic turbulence with the von Kármán spectra of temperature and wind velocity fluctuations. Furthermore, the transverse coherence function $\Gamma(x;y,z)$ of a plane sound wave propagating through an atmosphere with IGW was calculated. It was shown that $\Gamma(x;y,z)$ is an anisotropic function of the transverse coordinates y and z, while the coherence function for the von Kármán spectra of temperature and wind velocity fluctuations is an isotropic function of these coordinates.

Finally, note that the variances and correlation functions of log-amplitude and phase fluctuations of plane and spherical sound waves, and the transverse coherence function of a spherical sound wave can be readily calculated using the general formulas for these statistical moments obtained in Refs. 12–14 and Eq. (25) for the effective 3D spectral density, derived in the present paper.

ACKNOWLEDGMENTS

This article is partly based upon work supported by the U.S. Army Research Office Grant DAAG19-01-1-0640 and the Russian Foundation of Basic Research, Grant 03 05-04001.

[1] E. E. Gossard and W. H. Hoke, *Waves in the Atmosphere* (Elsevier, Amsterdam, 1975).
[2] R. B. Stull, *An Introduction to Boundary Layer Meteorology* (Kluwer, Dordrecht, 1988).
[3] D. C. Fritts, T. Tsuda, T. Sato, S. Fukao, and S. Kato, "Observational evidence of a saturated gravity wave spectrum in the troposphere and lower stratosphere," J. Atmos. Sci. **45**, 1741–1758 (1988).
[4] C. A. Hostetler and C. S. Gardner, "Observations of horizontal and vertical wave number spectra of gravity wave motions in the stratosphere and mesosphere over the mid-Pacific," J. Geophys. Res. **99**, 1283–1302 (1994).
[5] I. P. Chunchuzov, "On the high-wave number form of the Eulerian internal wave spectrum in the atmosphere," J. Atmos. Sci. **59**, 1753–1774 (2002).
[6] K. R. Allen and R. I. Joseph, "A canonical statistical theory of oceanic internal waves," J. Fluid Mech. **204**, 185–228 (1989).
[7] C. O. Hines, "Theory of the Eulerian tail in the spectra of atmospheric and oceanic internal gravity waves," J. Fluid Mech. **448**, 289–313 (2001).
[8] S. D. Eckermann, "Isentropic advection by gravity waves: Quasi-universal M^{-3} vertical wave number spectra near the onset of instability," Geophys. Res. Lett. **26**, 201–204 (1999).
[9] C. O. Hines, L. I. Childress, J. B. Kinney, and M. P. Sulzer, "Modeling of gravity-wave tail spectra in the middle atmosphere via numerical and Doppler-spread methods," J. Atmos. Sol.-Terr. Phys. **66**, 933–948 (2004).
[10] E. M. Dewan and R. E. Good, "Saturation and the 'universal' spectrum for vertical profiles of horizontal scalar winds in the atmosphere," J. Geophys. Res. **91**, 2742–2748 (1986).
[11] V. E. Ostashev, *Acoustics in Moving Inhomogeneous Media* (E&FN SPON, London, 1997).
[12] V. E. Ostashev and D. K. Wilson, "Log-amplitude and phase fluctuations of a plane wave propagating through anisotropic, inhomogeneous turbulence," Acust. Acta Acust. 87, No. 6, 685–694 (2001).
[13] V. E. Ostashev, D. K. Wilson, and G. H. Goedecke, "Spherical wave propagation through inhomogeneous, anisotropic turbulence: Studies of log-amplitude and phase fluctuations," J. Acoust. Soc. Am. **115**, 120–130 (2004).
[14] V. E. Ostashev and D. K. Wilson, "Coherence function and mean field of plane and spherical sound waves propagating through inhomogeneous anisotropic turbulence," J. Acoust. Soc. Am. **115**, 497–506 (2004).
[15] D. C. Fritts and P. K. Rastogi, "Convective and dynamic instabilities due to gravity wave motions in the lower and middle atmosphere: Theory and observations," Radio Sci. **20**, 1247–1277 (1985).
[16] A. S. Gurvich and I. P. Chunchuzov, "Parameters of the fine density structure in the stratosphere obtained from spacecraft observations of stellar scintillations," J. Geophys. Res. **108** (D5), ACL 6-1–ACL 6-4 (2003).

[17]J. A. Whiteway and T. J. Duck, "Evidence for critical level filtering of atmospheric gravity waves," Geophys. Res. Lett. **23**, 145–148 (1996).
[18]R. A. Vincent, S. J. Allen, and S. D. Eckermann, "Gravity wave parameters in the lower stratosphere," in *Gravity Wave Processes: Their Parameterization in Global Climate Models*, edited by K. Hamilton (Springer, Berlin, 1997), pp. 7–25.
[19]J. T. Bacmeister, S. D. Eckermann, A. Tsias, K. S. Carslaw, and T. Peter, "Mesoscale temperature fluctuations induced by a spectrum of gravity waves: A comparison of parametrization and their impact on stratospheric microphysics," J. Atmos. Sci. **56**, 1913–1924 (1999).
[20]E. M. Dewan, N. Grossbard, A. F. Queseda, and R. E. Good, "Spectral analysis of 10-m resolution scalar velocity profiles in the stratosphere," Geophys. Res. Lett. **11**, 80–83 (1984).
[21]C. O. Hines, "The saturation of gravity waves in the middle atmosphere. I. Critique of linear instability theory," J. Atmos. Sci. **48**, 1348–1359 (1991).
[22]*Atmospheric Turbulence and Air Pollution Modeling*, edited by F. T. M. Neuwstadt and Y. Van Dop (Reidel, London, 1982).
[23]I. P. Chunchuzov, "Influence of internal gravity waves on sound propagation in the lower atmosphere," Meteorol. Atmos. Phys. **85**, 61–76 (2004).
[24]J. Hinze, *Turbulence* (McGraw-Hill, New York, 1975).
[25]E. M. Salomons, *Computational Atmospheric Acoustics* (Kluwer Academic, Dordrecht, 2001).
[26]V. E. Ostashev and G. H. Goedecke, "Sound scattering cross section for von Kármán spectra of temperature and wind velocity fluctuations," in Proceedings 1997 Battlespace Atmospheric Conference, San Diego, 171–180 (1998).
[27]S. N. Kulichkov, "Long-range propagation and scattering of low-frequency sound pulses in the middle atmosphere," Meteor. Atmos. Phys. **85**, 47–60 (2004).
[28]E. H. Brown and F. F. Hall, "Advances in atmospheric acoustics," Rev. Geophys. Space Phys. **16**(1), 47–110 (1978).
[29]S. P. Singal, "Acoustic sounding stability studies," in *Encyclopedia of Environment Control Technology. V. 2: Air Pollution Control* (Gulf Publishing, Houston,1989), pp. 1003–1061.
[30]S. M. Rytov, Yu. A. Kravtsov, and V. I. Tatarskii, *Principles of Statistical Radio Physics. Part 4, Wave Propagation through Random Media* (Springer, Berlin, 1989).